

## Appendix 1

### Analysis of a mechanistic model

The minimal model used in this study is very simple. Particularly the growth of macrophytes is modelled in an extremely simple, phenomenological way, neglecting the seasonal cycle and complexities in the growth of macrophytes. In this appendix we used the individual-based model Charisma (Van Nes et al. 2002, 2003) to check the robustness of the results. Though this model describes macrophyte growth in a detailed mechanistic way, it still uses a phenomenological approach to describe the clearing effect of macrophytes. For a full mechanistic approach we would need to add nutrients, phytoplankton, zooplankton and wind resuspension in a dynamical way, making the model very complex, while there is ample empirical evidence that macrophytes cause clear water in shallow lakes (Scheffer 1989). To include advection and dispersion of water, we slightly adapted the model and modelled the vertical light attenuation in a dynamical way. We used the parameter settings of *Chara aspera* as an example of a species that potentially has a strong effect on the water turbidity (Van Nes et al. 2002).

#### Model description Charisma

The individual-based model Charisma is described in detail elsewhere (Van Nes et al. 2002, Van Nes et al. 2003), here we merely give an overview of the main features.

Charisma was designed as a multi-species model of submerged plants, but was applied here for only one species. Spatial processes can be included in the model by defining a grid of cells in which the plants grow. Here we used either one cell or a single row of 100 cells to model a chain of lakes or a river. Each cell has its own environmental features (bicarbonate, depth, vertical light attenuation coefficient), a seed bank with two types of overwintering structures (in case of *C. aspera* oospores and bulbils) and contains a collection of super individuals (Scheffer et al. 1995) of macrophytes (i.e. individuals that keep also track of the number that they represent). The integration step of Charisma is one day, but within each day the photosynthetic rate is computed as a function of the daily light variation by a three-point Gaussian integration (Goudriaan 1986). The seasonal cycle of macrophytes is included in the model. A part of the vegetation biomass survives the winter as overwintering structures in the seed bank. At a fixed day, growth is initiated by transforming part of the seeds and tubers in each grid cell into young sprouts.

Daily growth of each individual of the plants depends on photosynthesis and respiration. Respiration is modelled as a simple basal metabolism that is exponentially dependent on temperature. The per-capita photosynthesis is modelled as a factor  $P_{\max}$  that is limited by temperature  $T$ , light in the water column  $I_w$ , bicarbonate  $B$  and senescence as distance  $D$  to the growth tip.

$$P = P_{\max} f(T, I_w, B, D) \quad (\text{A1-1})$$

The effect of each factor is formulated as a simple Monod saturation function with the exception of the saturation function of temperature, for which a sigmoid saturating function is used. A fixed part of the daily production is invested in roots and overwintering structures. These structures do not contribute to primary production. The length of young plants increases proportionally with their biomass keeping a fixed weight per meter sprout till they reach their maximum length or the water surface, further growth causes a proportional increase over the whole length of the plants.

Three mortality causes are explicitly included in the model: wave damage, mortality due to competition at high plant densities and seasonal die off. All these mortalities cause the number of individuals to decrease. At the end of the season all above-ground biomass dies off, while the biomass that was reserved for overwintering structures is transferred to the seed bank.

Most environmental factors are modelled as external variables. In the original model a quasi-steady state approach was used for the vertical light attenuation. Many studies show that plants reduce turbidity in various ways (Scheffer 1998). We used the experimentally determined Monod equation to describe the reduction of the light attenuation coefficient ( $K_p$ ) as a function of the total biomass ( $\sum B$ ) in each grid cell ( $K_d$ : the vertical light attenuation coefficient, which is varied between 1 and 8,  $H_K$ : half-saturation constant)

$$K_p = K_b + (K_d - K_b) \frac{H_K}{\sum B + H_K} \quad (\text{A1-2})$$

Parameter values used were:  $K_b=0.5 \text{ m}^{-1}$ ,  $H_K=40 \text{ g ash free dry weight m}^{-2}$ . Equation A1-2 shows that vegetation cannot reduce light attenuation below the background light attenuation  $K_b$ .  $H_K$  is an experimentally determined parameter.  $K_p$  was calculated daily for each grid cell.

In this study we interpreted  $K_p$  as the carrying capacity of a logistic growth function with a growth rate  $r$ :

$$\frac{dK_i}{dt} = r K_i \left( 1 - \frac{K_i}{K_p} \right) + a (K_{i-1} - K_i) + \text{dispersion} \quad (\text{A1-3})$$

The advection term was modeled in a similar way as in the minimal model. The dispersion was set to zero. The first cell got a fixed water with a fixed vertical light attenuation. We used a growth rate of  $0.5 \text{ d}^{-1}$  and solved this differential equation with an Euler scheme with a step size of  $0.2 \text{ d}$ . All other parameters were taken from Van Nes et al. (2002) (see Table 1 in that publication).

The range with alternative stable states is analysed by changing the external vertical light attenuation step by step while letting the

model stabilize. First the vertical light attenuation is increased step by step and subsequently decreased. Only the summer biomass is plotted (for details see Van Nes et al. 2002).

## Results

First we analysed the effect of flushing on the range with alternative stable states in a single cell. If we introduce flushing in this situation, the range with alternative stable states is reduced (Fig. A1-1), similarly to the minimal model (cf. Fig. 2).

We then analysed a chain of 100 sections in Charisma. The results of Charisma were qualitatively very similar as compared with the minimal model. Both a travelling wave (Fig. 4), and a steep gradient in space (Fig. 5, 6) were reproduced in Charisma with realistic parameters (Fig. A1-2, A1-3, A1-4). The time scale of the Charisma results was however much longer, probably due to time lags in the production of reproductive organs.

Figure A1-4 only showed a less delayed gradient than in the minimal model (Fig. 6). Another interesting difference with the

minimal model is that the growth rate of algae was now affecting the results. With a slower algal growth rate the clearing effect of macrophytes became less effective (as the biomass of macrophytes had a seasonal cycle now).

## References

- Goudriaan, J. 1986. A simple and fast numerical method for the computation of daily totals of crop photosynthesis. – *Agric. For. Meteorol.* 38: 249–254.
- Scheffer, M. 1998. *Ecology of shallow lakes*. – Chapman and Hall.
- Scheffer, M. et al. 1995. Super-individuals a simple solution for modelling large populations on an individual basis. – *Ecol. Modell.* 80: 161–170.
- Van Nes, E. H. et al. 2002. Dominance of charophytes in eutrophic shallow lakes-when should we expect it to be an alternative stable state? – *Aquat. Bot.* 72: 275–296.
- Van Nes, E. H. et al. 2003. Charisma: a spatial explicit simulation model of submerged macrophytes. – *Ecol. Modell.* 159: 103–116.

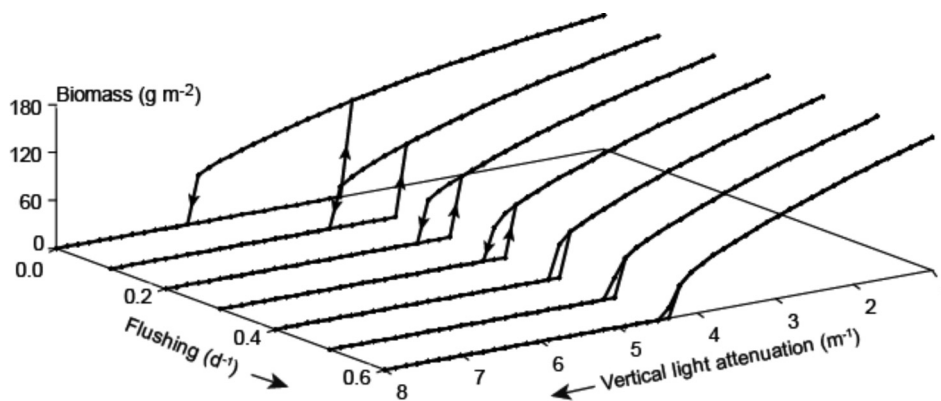


Figure A1-1. The equilibrium summer biomass of submerged vegetation (2 July) and vertical light attenuation in a single shallow lake computed in Charisma as a function of the vertical light attenuation with different flushing rates (a). Hysteresis disappears with increasing flushing.

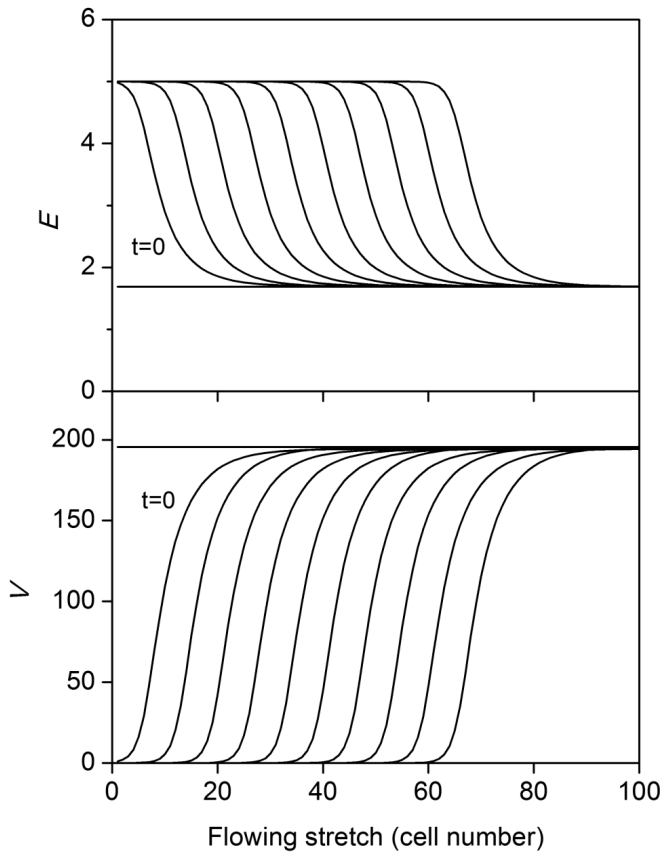


Figure A1-2. Movement of the location of the shift from the turbid to the vegetated equilibrium in time along a river stretch consisting of 100 lake cells (computed from the adapted Charisma model using default values and  $E_0 = 5$ ,  $E_{in} = 5$ ,  $a = 2$ ). Different lines represent the state of the system at different times (all at 1 September, with 10 years between each,  $t = 0$  also included).

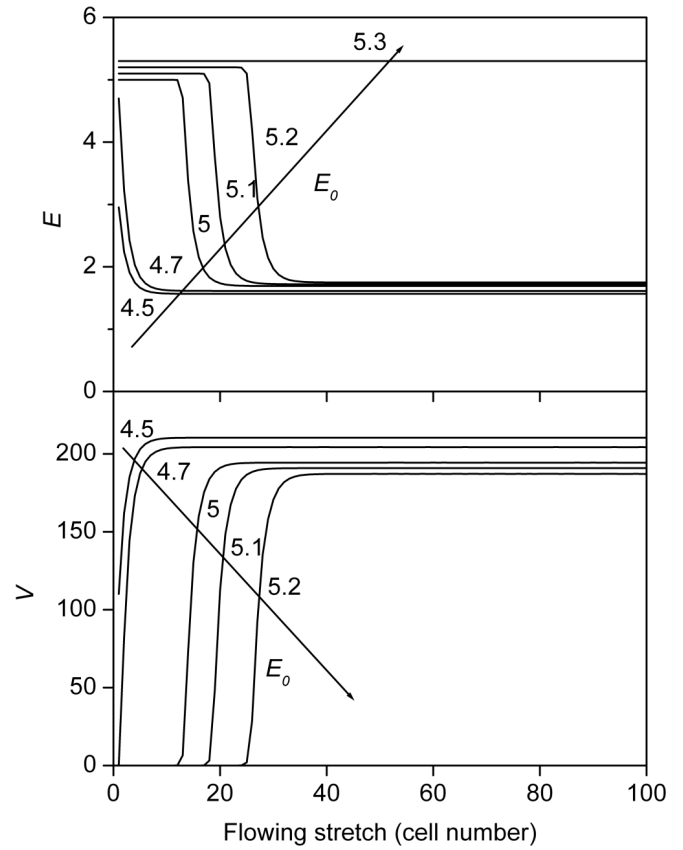


Figure A1-3. Turbidity ( $E$ ) and abundance of submerged vegetation ( $V$ ) along a river stretch with 100 cells with increasing turbidity of non-vegetated water ( $E_0$ ) from 3 to 5.2 (indicated by arrows) computed from the adapted Charisma model (for  $a = 0.5$ ) after 100 years of stabilizing.

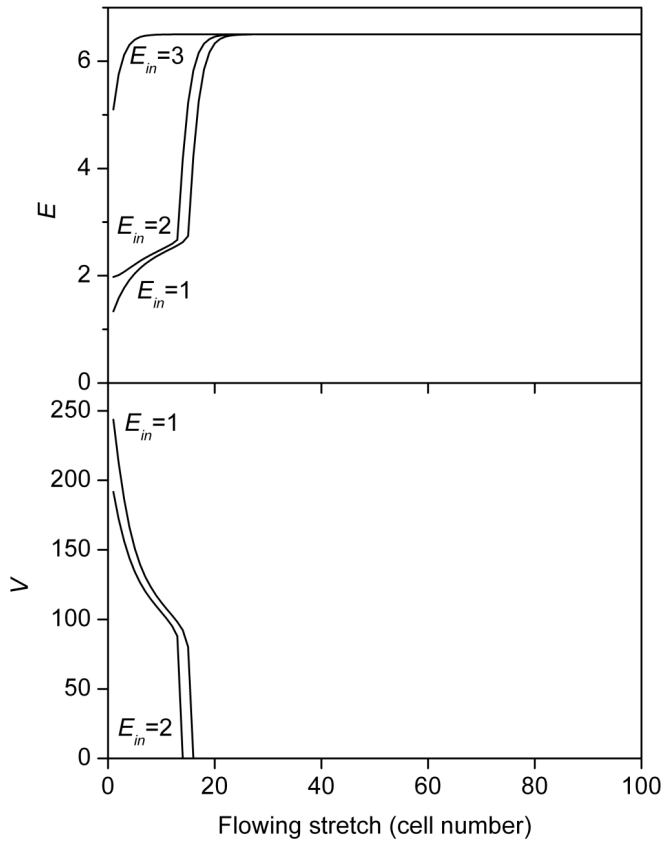


Figure A1-4. Turbidity (E) and abundance of submerged vegetation (V) along a river stretch with 100 cells with different turbidity of incoming water ( $E_{in}$ ) computed from the adapted Charisma model (for  $a = 0.5$ ,  $E_0 = 7$ ).

## Appendix 2

### The effects of dispersion and water depth

Continuous advection of discrete well-mixed sections causes some dispersion (i.e. mass transfer driven by a concentration gradient). This dispersion is due to the fact that each section is considered well-mixed and that it is continuously exchanging to neighbor cells, which results in variation in water velocity. This dispersion seems realistic if we model a chain of mixed lakes; however, if the sections are arbitrarily chosen and not well mixed, this dispersion can be considered as a model artifact (Rood 1987). However, we think that in systems such as lowland rivers, real dispersion is usually even stronger than the numerical dispersion because many other factors, such as water turbulence or differences in water velocity cause dispersion.

### Method

We tested the effect of such stronger dispersion by adding a dispersion term to model 2 resulting in model 3:

$$\frac{dE_i}{dt} = r_e E_i \left( 1 - \frac{E_i}{f_e(V_i)} \right) + a (E_{i-1} - E_i) + D(E_{i-1} - 2E_i + E_{i+1}) \quad (\text{A2-1})$$

$$\frac{dV_i}{dt} = r_v V_i \left( 1 - \frac{V_i}{f_v(E_i)} \right) \quad (\text{A2-2})$$

We also analysed the effect of water depth by changing the parameter  $h_E$  in the model. This parameter represents the critical turbidity where the lake becomes vegetated and is considered to be related to the average water depth.

## Results

Lake chains with a rather long water retention time (low flushing rate) or rivers with a low flowing velocity (proportional to the flushing rate) may also exhibit hysteresis for a certain range of initial turbidities  $E_0$  depending on the parameter  $h_E$  (Fig. A2-1A, A2-2A). Due to the inverse relationship between  $h_E$  and water depth, alternative states are more likely at higher  $h_E$  and thus, in shallower water (Fig. A2-1A). With decreasing retention time in lake chains or increasing flowing velocity in rivers and thus higher flushing rate  $a$ , the range with alternative stable states becomes smaller and finally disappears above a certain  $a$ , but abrupt shifts between macrophyte and phytoplankton dominance may still occur along the lake chain or river section (spatial shift) (Fig. A2-1B, A2-2A). The range of  $h_E$  with alternative states or spatial shifts is moved to higher values with increasing  $a$  at a given  $E_0$ . Alternative states only occur for flushing rates ( $a$ ) up to about 1 (Fig. A2-2A).

Increasing dispersion only had a rather small effect on the critical thresholds, but all shifts became smoother. Dispersion slightly decreases the range of alternative states, but adds a range with spatial shifts (Fig. A2-1C, A2-2B). At lower retention times or higher flowing velocities, considering dispersion results in a broader range of conditions for spatial shifts from phytoplankton to macrophyte dominance along the lake chain or river stretch, but does not influence the thresholds for shifts to phytoplankton dominance (Fig. A2-1D, A2-2B). The range for the occurrence of alternative stable states is smaller for  $E_0$ , but slightly higher for  $a$  (up to 1.3) with dispersion (Fig. A2-2B).

## References

- Rood, R. B. 1987. Numerical advection algorithms and their role in atmospheric transport and chemistry models. – *Rev. Geophys.* 25: 71–100.

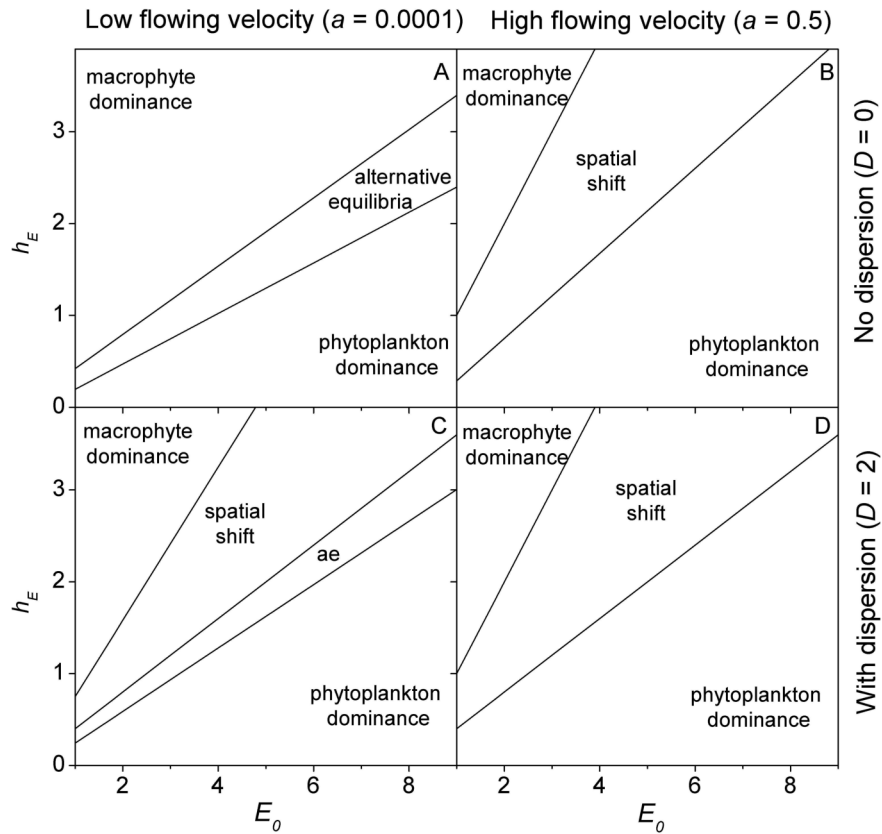


Figure A2-1. The effect of flushing rate and dispersion on the occurrence of vegetation dominance, two alternative spatial stable states or phytoplankton dominance in response to turbidity of non-vegetated water ( $E_0$ ) in a river stretch consisting of 100 lake cells depending on the parameter  $h_E$ . (A) low flushing rate ( $a = 0.0001$ ) without dispersion; (B) high flushing rate ( $a = 0.5$ ) without dispersion; (C) low flushing rate with dispersion ( $D = 2$ ); (D) high flushing rate with dispersion. Definitions: vegetation dominance,  $V(\text{last cell}) > 0.3$ ; phytoplankton dominance,  $V(\text{last cell}) < 0.3$ ; and spatial shift,  $|V(\text{last cell}) - V(\text{first cell})| > 0.3$ .

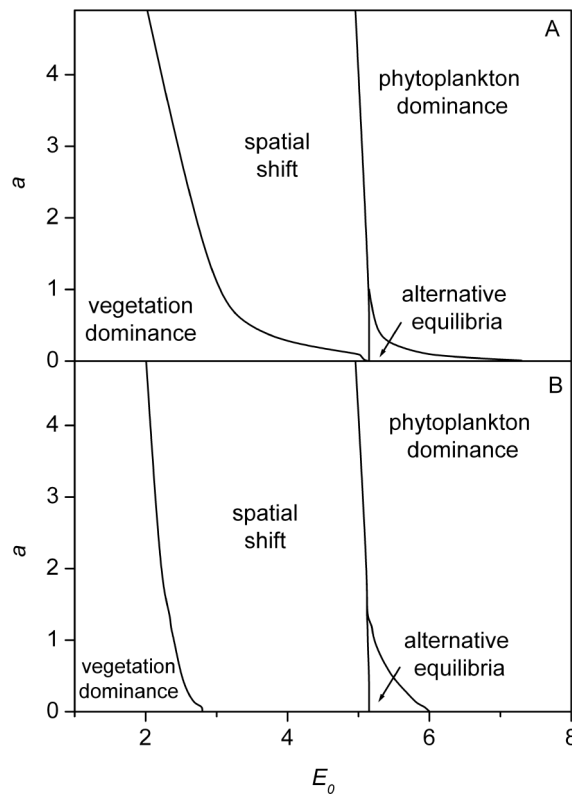


Figure A2-2. Two-dimensional bifurcation plot showing the occurrence of vegetation dominance, alternative stable equilibria or phytoplankton dominance in response to turbidity of non-vegetated water ( $E_0$ ) in a river stretch consisting of 100 lake cells depending on flushing rate ( $a$ ) (for default value  $h_E = 2$ ). (A) without dispersion (model 2) and (B) with dispersion (model 3).